TABLE I
COMPARISON OF MEASURED AND CALCULATED PARAMETERS

Depth of Overlap 'd' (mm)	Main Cavity Frequency (MHz)		Main to Side Cavity Coupling	
	Measured	Calculated	Measured	Calculated
6	2997.85	2994.96	0.0127	0.0111
7.6	2991.79	2988.16	0.0216	0.0204
8.6	2987.55	2984.69	0.0282	0.0281
9.2	2984.15	2982.94	0.0321	0.0335

IV. CALCULATIONS AND RESULTS

To evaluate the inter-cavity coupling constant one has to first evaluate the fields at the center of the ellipse by which the aperture is represented. We do this by using the finite element routine developed in [7]. The computed values of the frequency of the main cavity (with the aperture on its wall), and the intercavity coupling constant are given in Table I for different sizes and positions of the iris as determined by the depth of overlap d. Along with these the corresponding experimental values are also given. The uncut resonant frequency of the main cavity used for generating Table I was 3006.7 MHz. Earlier we only had the experimental technique. The new aspect is our ability to predict the values. The prediction is precise enough for our needs during the initial design stage. Thus, we have been able to simplify the design process.

REFERENCES

[1] D. E. Nagle, E. A. Knapp, and B. C. Knapp, "Coupled resonator model for standing wave accelerator tanks," *Rev. Sci. Instr.*, vol. 38, p. 1583, 1967.

[2] E. A. Knapp, B. C. Knapp, and J. M. Potter, "Standing wave high energy linear accelerator structures," *Rev. Sci. Instr.*, vol. 39, p. 979, 1968.

[3] O. Shanker, P. A. Rai Chowdhuri, and R. Verma, "Coupling coefficient information from the linac mode spectrum," *Rev. Sci. Instr.*, vol. 60, p. 3301, 1989.

[4] O. Shanker, "Matrix analysis of coupled cavity structures," in *Proc. Int. Conf. on Millimeter Waves and Microwaves,* Dehra Dun, India, Dec. 1990, Tata McGraw Hill, New Delhi, p. 620.

[5] ——, "Generalization of linac mode spectrum and fitting procedure," *Rev. Sci. Instr.*, vol. 63, p. 4443, 1992.

[6] H. C. Hoyt, D. D. Simmonds, and W. F. Rich, "Computer designed 805 MHz proton linac cavities," *Rev. Sci. Instr.*, vol. 37, p. 755, 1966.

[7] R. Roy and O. Shanker, "Evaluation of microwave linac cavity field and parameters by the finite element method," *Indian J. Pure and Applied Physics,* vol. 30, p. 207, 1992.

[8] H. A. Bethe, "Theory of diffraction by small holes," *Phys. Rev.*, vol. 66, p. 163, 1944.

[9] R. E. Collin, *Field Theory of Guided Waves.* New York: McGraw-Hill, 1960.

[10] E. Jahnke and F. Emde, *Tables of Functions,* 4th ed., New York: Dover, 1945, p. 58.

Shape Function Optimization in the Finite Element Analysis of Waveguides

H. E. Hernández-Figueroa and G. Pagiatakis

***Abstract*—In this paper, a novel finite element technique is presented, which can substantially reduce the computational effort required for the analysis of waveguide structures. Demonstrative examples, whose finite element solutions are obtained by combining this technique with two well-known formulations—$E_z - H_z$ and H-field—are given.**

I. INTRODUCTION

A drawback of the finite element method when applied to modal waveguide analysis is the extensive use of computer resources: memory space and time. Although the order of the resulting matrix eigenvalue problem mainly depends on the geometry of the specific structure analyzed, the kind of mesh adopted, and the formulation used, most of these problems demand a large amount of data manipulations. However, substantial reduction of the computational effort can be achieved by taking advantage of the Rayleigh–Ritz Principle (RRP), which is the basis of the α-finite element technique [1]–[3]. This technique was first introduced by Laura and co-workers (see [1] and references therein) who used modified basis functions for the bilinear quadrilateral (Q_1) elements applied to the *scalar* 2-D Helmholtz equation. In [2], novel basis functions were introduced to deal with the versatile linear triangular (P_1) elements, and applied to the *vectorial* $E_z - H_z$ formulation [4]. Also, in that reference, the performances of those two sets of basis functions were compared, and the results showed almost no differences in terms of accuracy. However, as the modified P_1 functions provide close analytical expressions for the integrals associated with the elements of the elementary matrices, these functions are much more attractive than the Q_1 ones, which instead require the use of numerical integration schemes, and therefore, more CPU time.

In this paper, the P_1-α-finite element technique is presented, and the conditions for combining with finite element formulations for the analysis of waveguide structures are discussed. Also, the feasibility of such combined approaches is demonstrated by making use of the widely known $E_z - H_z$ and H-field [5] formulations, applied to the analysis of hollow and dielectric-loaded metallic waveguides which possess analytical solutions [6].

II. THE P_1-α-FINITE ELEMENT TECHNIQUE

This technique, contrary to the common practice of increasing the mesh size or the basis function order, minimizes the discretization error, for a given mesh, by taking advantage of the RRP. According to this principle, the approximate eigenvalues λ_i', obtained by solving the resulting matrix eigenvalue problem $Ax = \lambda Bx$, where A and B are Hermitian and B is positive definite, are always upper bounds

Manuscript received August 4, 1992; revised December 7, 1992. This work was supported by the Brazilian Agency CAPES and the State Scholarship Foundation of Greece (IKY).

H. E. Hernández-Figueroa was with the Laser Optics Group, Department of Physics, Imperial College, London, SW7 2BZ, U.K. He is now with the Department of Electronic and Electrical Engineering, University College London, Torrington Place, London WC1E 7JE, U.K.

G. Pagiatakis is with the Department of Electrical Engineering, Imperial College, London, SW7 2AZ, U.K.

IEEE Log Number 9209353.

for the exact eigenvalues λ_i', that is, $\lambda_i \leq \lambda_i'$. This suggests the introduction of an extra parameter in the finite-element scheme, say α, such that λ_i' becomes a function of α: $\lambda_i' \rightarrow \lambda_i''(\alpha) = ((x^T(\alpha)A(\alpha)x(\alpha))/((x^T(\alpha)B(\alpha)x(\alpha))$. Thus, $\lambda_i''(\alpha)$ can be minimized in order to reach closer values to λ_i. If that minimum occurs for $\alpha = \alpha_{\text{opt}}$, then according to the RRP, $\lambda_i \leq \lambda_i''(\alpha_{\text{opt}}) \leq \lambda_i'$.

In order to meet the requirements of the RRP, we introduce the parameter α as an exponential factor in the conventional P_1 basis functions [7], yielding the following set of suitable modified local shape functions [2], [3]:

$$\Psi_1 = 1 - (\xi + \eta)^\alpha \tag{1a}$$

$$\Psi_2 = 1 - (1 - \xi)^\alpha \tag{1b}$$

$$\Psi_3 = 1 - (1 - \eta)^\alpha \tag{1c}$$

where the coordinates (ξ, η) are related to the so-called master finite element [7], $\hat{e}$, which is a triangle with vertices located at $(0,0)$, $(1,0)$, and $(0,1)$. The conventional set of P_1 local shape functions is obtained by replacing $\alpha = 1$. Also, when $\alpha > 1$, those modified functions are concave and, therefore, more suitable for solving second-order differential operators [2] than the conventional ones.

On the other hand, we observe that the elements of the elementary matrices [7] of probably all the finite element formulations available for waveguide analysis, apart form constants, can be expressed in terms of the following three equivalent kinds of exact integrals [2], [3]:

$$\begin{aligned}\int_{\hat{e}} (\xi+\eta)^p (1-\xi)^q \, d\xi \, d\eta &= \int_{\hat{e}} (\xi+\eta)^p (1-\eta)^q \, d\xi \, d\eta \\ &= \int_{\hat{e}} (1-\xi)^p (1-\eta)^q d\xi \, d\eta \\ &= 1/((p+1)(q+1)) \\ &\quad - \Gamma(p+1)\Gamma(q+1)/ \\ &\quad \Gamma(p+q+3) \\ p, q > -1 \end{aligned} \tag{2}$$

where p, q are real functions of α, and $\Gamma(x)$ represents the Gamma function. Thus, all the terms of such modified elementary matrices can be written as the product of the conventional ones times very simple analytical α-dependent factors which assume the value one when α is set to one. Consequently, the implementation of this technique in the conventional finite element formulations requires neither additional numerical integrations nor extra memory space.

III. Numerical Results

First, we analyzed the TE_{11}/TM_{11} modes of the hollow metallic rectangular guide shown in cross section in Fig. 1(a). For both

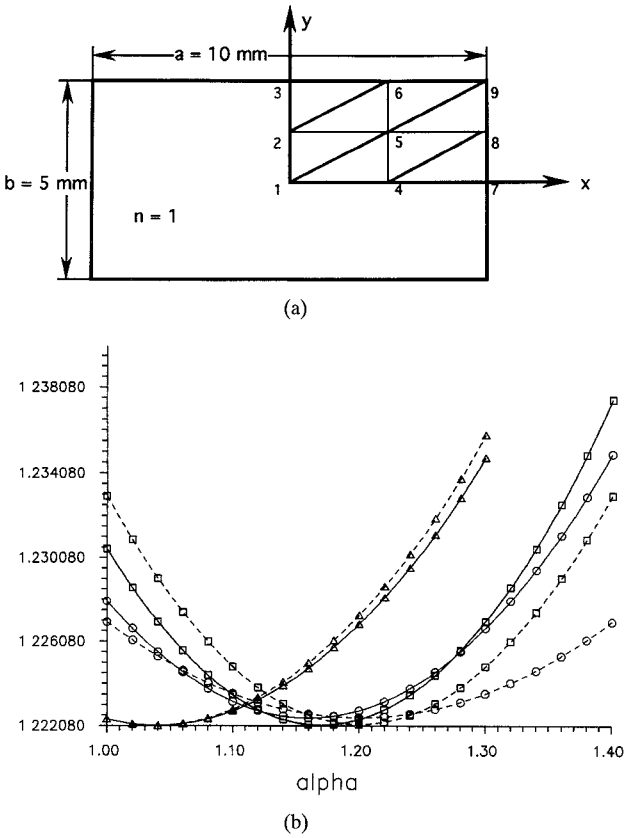

Fig. 1. (a) The cross section of the hollow metallic rectangular waveguide and 2×2 mesh. (b) k_0 versus α. $E_z - H_z$ and H-field formulations: solid and dashed curves, respectively; 7×2 mesh (squares), 4×4 mesh (circles), and 11×11 mesh (triangles).

formulations, the propagation constant β was set equal to 1 mm^{-1}. In addition, in order to facilitate the comparison, for the $E_z - H_z$ formulation, the effective propagation constant $\beta_{\text{eff}} = \beta/k_0$ was set to $1/1.222080$, where the exact value of k_0 (wave number in vacuum) $k_0 = 1.222080$ mm^{-1} was adopted. Fig. 1(b) illustrates the variation of the calculated k_0 versus the parameter α for three different meshes, and the numerical results are listed in Table I. In all cases, there exists an optimum value of $\alpha = \alpha_{\text{opt}}$ at which the finite elements solution of $k_0(\alpha)$ is minimized and approaches the exact value. Table I shows that for a given mesh, the accuracy can be substantially improved. For instance, a 7×2 mesh yields a substantial accuracy improvement: form 0.694% to 0.002%, and from 0.93% to 0.005%, for the $E_z - H_z$ and H-field formulations, respectively. Table I also shows that an 11×11 mesh with $\alpha = 1$ offers the

TABLE I
Results for the Hollow Metallic Rectangular Waveguide

		$\alpha = 1$		$\alpha = \alpha_{\text{opt}}$		
Formulation	Mesh	k_0 (mm^{-1})	Error (%)	k_0 (mm^{-1})	Error (%)	α_{opt}
$E_z - H_z$	7×2	1.230516	0.694	1.222111	0.002	1.17
	4×4	1.228005	0.485	1.222434	0.029	1.16
	11×11	1.222426	0.028	1.222100	0.002	1.04
H-Field	7×2	1.233446	0.930	1.222146	0.005	1.20
	4×4	1.226613	0.371	1.222459	0.031	1.20
	11×11	1.222428	0.028	1.222097	0.001	1.04

same accuracy as a 4×4 mesh with $\alpha = \alpha_{opt}$. Consequently, in this example, the number of unknowns was reduced by a factor of 7.5, and the CPU time, including three iterations to determine α_{opt}, was reduced by a factor of 10. The method adopted for solving the matrix eigenvalue problem was the subspace iteration.

Second, we analyzed the fundamental mode of the dielectric-loaded metallic rectangular waveguide shown in cross section in Fig. 2(a). For both formulations, we assumed $\beta = 1\ \text{mm}^{-1}$. However, in addition, for the $E_z - H_z$ formulation we assumed $\beta_{eff} = 1/0.808724$, where the exact value $k_0 = 0.808724\ \text{mm}^{-1}$ was adopted. Fig. 2(b) illustrates the variation of k_0 versus the exponential parameter α, for three different meshes, and the related numerical results are listed in Table II. Again, the values obtained using $\alpha = \alpha_{opt}$ are closer to the exact solution than the conventional ones obtained with $\alpha = 1$. Table II shows, for instance, that the same accuracy can be obtained by using either a 10×6 mesh with $\alpha = 1$, or a 7×4 mesh with $\alpha = \alpha_{opt}$. Consequently, the number of unknowns was reduced by a factor of 2, and the CPU time, including three iterations, was reduced by a factor of 1.5.

The curves representing the dependence of k on α, show a very regular behavior with a well-defined minimum. Consequently, this makes the calculation of α_{opt} very easy—no more than six attempts were necessary in all the situations analyzed. However, this number can be reduced to only three, by noticing that such curves can be very well fitted by quadratic ones of the kind $k(\alpha) = A_1 + A_2 + A_3\alpha^2$, where $A_{1,2,3}$ are coefficients to be determined.

Although in almost all the situations it is possible to reduce the number of unknowns, there will be cases in which even that reduced number can be quite large. The consequence of this is that the need of at least three iterations to calculate α_{opt} can make the present technique more CPU time consuming than the conventional finite element method ($\alpha = 1$).

However, the drawback mentioned above can still be overcome by the present technique. Extensive numerical experiments have shown that for a given mode, the variations of α_{opt} and $k(\alpha_{opt})$ are practically negligible for all points of the associated dispersion curve [2]. Typical variations are less than 0.5% and 0.01% for α_{opt} and $k(\alpha_{opt})$, respectively. Therefore, one needs to calculate α_{opt} only once. The rest of the curve can be determined by using the same α_{opt}, almost maintaining the same improved accuracy. Consequently, even if the reduced number of unknowns is significant, it is still possible to obtain a reduction in CPU time, which would be, in fact, proportional to the number of points required to determine the dispersion curve.

Finally, the results of the situations so far analyzed show that the optimization of α also improves the accuracy of the fields representation.

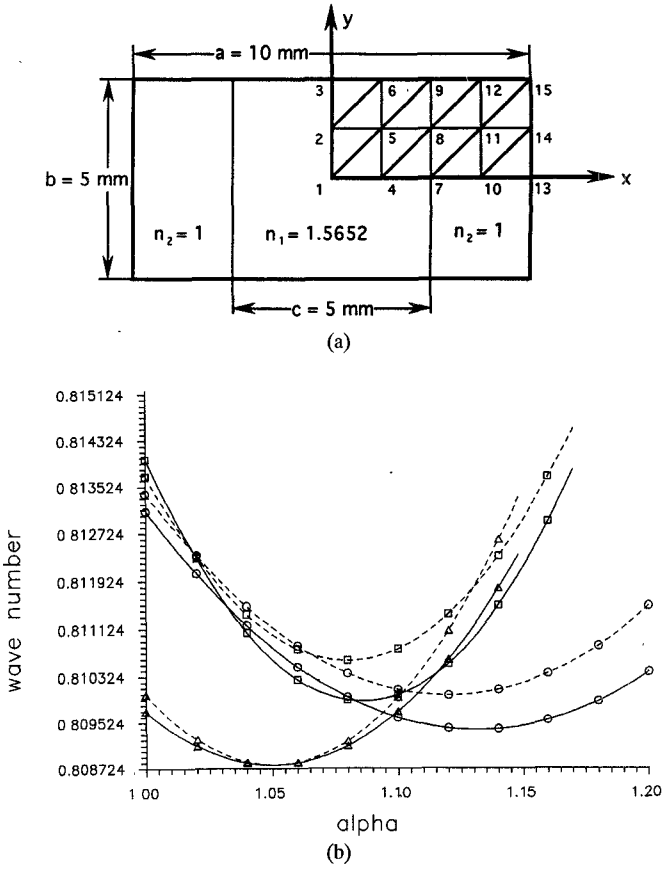

Fig. 2. (a) The cross section of the dielectric-loaded metallic rectangular waveguide and 4×2 mesh. (b) k_0 versus α. $E_z - H_z$ and H-field formulations: solid and dashed curves, respectively; 6×4 mesh (squares), 7×4 mesh (circles), and 10×6 mesh (triangles).

IV. Conclusions

In this paper, the P_1-α technique has been presented to be capable of being combined with virtually any available finite element formulation. The results obtained show that a substantial reduction in the number of unknowns, and consequently CPU time, can be achieved. In principle, this technique should be also useful for the analysis of optical waveguides. However, its application to nonlinear waveguide problems, where the nonlinear iterations increase the computational effort considerably, is particularly recommended.

TABLE II
Results for the Dielectric-Loaded Metallic Rectangular Guide

		$\alpha = 1$		$\alpha = \alpha_{opt}$		
Formulation	Mesh	k_0 (mm^{-1})	Error (%)	k_0 (mm^{-1})	Error (%)	α_{opt}
$E_z - H_z$	6×4	0.813998	0.652	0.809910	0.147	1.09
	7×4	0.813101	0.541	0.809400	0.083	1.13
	10×6	0.809717	0.086	0.808785	0.007	1.05
H-Field	6×4	0.813671	0.612	0.811066	0.289	1.08
	7×4	0.813397	0.578	0.810015	0.160	1.12
	10×6	0.810009	0.159	0.808789	0.008	1.05

ACKNOWLEDGMENT

The authors would like to thank Dr. A. Fernández and Dr. K. D. Leaver for helpful discussions.

REFERENCES

[1] J. C. Utjes, G. S. Sarmiento, and P. A. A. Laura, "Nonlinear optimization of the shape functions in the finite element method when determining cut-off frequencies of arbitrary cross section," *IEEE Trans. Microwave Theory Tech.*, vol. MTT-36, pp. 151–152, Jan. 1988.

[2] H. E. Hernández-Figueroa, "Optimized finite elements for solving the Helmholtz 2-D eigenvalue problem," M.Sc. thesis, Dep. Informatics, Pontifical Catholic Univ., Rio de Janeiro, Brazil, 1988 (in Portuguese).

[3] H. E. Hernández-Figueroa and G. Pagiatakis, "Size reduction of the H-field finite element formulation for waveguide structure analysis," in *Proc. IEE Int. Conf. Computat. Electromagn.* (London), Nov. 1991, pp. 272–275.

[4] Z. J. Csendes and P. Silvester, "Numerical solution of dielectric loaded waveguides: I—Finite-element analysis," *IEEE Trans. Microwave Theory Tech.*, vol. MTT-12, pp. 1124–1131, Dec. 1970.

[5] B. M. A. Rahman and J. B. Davies, "Finite-element analysis of optical and microwave waveguide problems," *IEEE Trans. Microwave Theory Tech.*, vol. MTT-32, pp. 20–28, Jan. 1984.

[6] R. E. Collin, *Field Theory of Guided Waves.* New York: McGraw-Hill, 1960.

[7] E. B. Becker, G. F. Carey, and T. Oden, *Finite Elements. An Introduction,* Vol. I. Englewood Cliffs, NJ: Prentice-Hall, 1981.